

# Quantum Scattering Calculations of the $\text{H} + \text{O}_2 \rightarrow \text{O} + \text{OH}$ Reaction<sup>†</sup>

Renat A. Sultanov and N. Balakrishnan\*

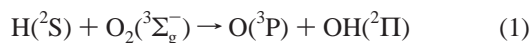
Department of Chemistry, University of Nevada Las Vegas, 4505 Maryland Parkway,  
Las Vegas, Nevada 89154

Received: February 25, 2004; In Final Form: April 8, 2004

We report quantum mechanical calculations of the  $\text{H} + \text{O}_2 \rightarrow \text{OH} + \text{O}$  reaction for total angular momentum quantum number  $J = 0$  in the absence of recombination. Our calculations employ two different potential energy surfaces—the widely used semiempirical double many-body expansion (DMBE IV) potential surface of Pastrana et al. (*J. Phys. Chem.* **1990**, *94*, 8073) and an ab initio potential surface by Troe and Ushakov (*J. Chem. Phys.* **2001**, *115*, 3621) which is yet to be tested against detailed quantum dynamics calculations. We explore the sensitivity of the dynamics to details of the potential energy surface. The reaction is dominated by narrow resonances due to the formation of the  $\text{HO}_2$  radical, and results are sensitive to details of the potential energy surfaces. Thermal rate coefficients evaluated using a  $J$ -shifting approximation differ by about 50% on the two potential surfaces. Calculations show that, within the  $J$ -shifting approximation, the Troe–Ushakov potential surface yields rate coefficients that are in better agreement with experiments.

## I. Introduction

One of the most important reactions in combustion chemistry is



It is the rate-limiting step in the combustion of hydrocarbons and flame propagation processes, and it continues to be the subject of a large number of experimental<sup>1–6</sup> and theoretical investigations.<sup>7–33</sup> The presence of two heavy oxygen atoms, long-range dipole–quadrupole and quadrupole–quadrupole interactions in the  $\text{O} + \text{OH}$  channel, and the deep potential well corresponding to the formation of the bound  $\text{HO}_2$  species make accurate theoretical calculations challenging. Quasibound states of the  $\text{HO}_2$  radical give rise to numerous scattering resonances in the energy dependence of the reaction probability, and accurate reproduction of the resonances is a challenging aspect of quantum dynamics calculations.

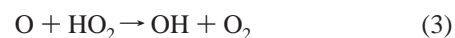
Theoretical studies of (1) include quasiclassical trajectory (QCT) calculations<sup>7–17</sup> and time-independent<sup>18–23</sup> and time-dependent<sup>24–33</sup> quantum-mechanical methods. The zero-point energy issue is a main problem in QCT calculations of this system.<sup>7,9</sup> The time-independent quantum approaches include both direct calculations of the cumulative reaction probability (CRP)<sup>22</sup> as well as state-resolved reaction probabilities<sup>18,19,23</sup> for total angular momentum quantum number  $J = 0$ . The quantum calculations by Pack et al.<sup>19</sup> for  $J = 0$  using hyperspherical coordinates still remain the benchmark state-to-state dynamics study of this system. Miller and co-workers<sup>21,22</sup> carried out direct calculation of the cumulative reaction probabilities for  $J = 0$  and invoked a  $J$ -shifting approach to compute thermal rate coefficients. Though the  $J$ -shifting approximation is questionable for this system full quantum calculations for higher values of  $J$  are computationally daunting.

Quantum calculations for selected  $J > 0$  values have been performed by Meijer and Goldfield<sup>30,31</sup> using the time-dependent wave packet method. Reaction cross sections from their calculations<sup>30</sup> were found to be significantly lower than the measured values, and this was attributed to uncertainties in the potential energy surface or nonadiabatic effects that were not included in the calculations. These calculations were not extended to evaluate the rate coefficients due to the large number of  $J$  values required. Because  $J > 0$  calculations for this system require massive computational effort, we believe that such calculations will be meaningful only when the underlying potential surfaces are accurately known. However,  $J > 0$  calculations even on approximate PES are very useful in determining the accuracy of approximate methods.

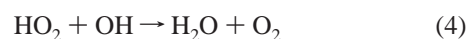
The reverse reaction



has also received considerable attention in recent years due to its role in odd hydrogen ( $\text{H}$ ,  $\text{OH}$ ,  $\text{HO}_2$ ) chemistry in the upper stratosphere and mesosphere.<sup>35–39</sup> Since hydroxyl radical is a catalytic destroyer of ozone in the upper stratosphere and mesosphere, the chemistry of hydroxyl radical in the upper atmosphere has come under much scrutiny. Reaction 2 along with



control the  $\text{OH}/\text{HO}_2$  branching in the upper stratosphere and mesosphere.  $\text{HO}_x$  is destroyed by reactions in which  $\text{HO}_2$  recombines with  $\text{H}$  and  $\text{OH}$ :



and



Accurate evaluations of rate coefficients for (2)–(4) at mesospheric temperatures are still a challenging problem. The

<sup>†</sup> Part of the “Gert D. Billing Memorial Issue”.

\* Corresponding author. Fax: (702)895-4072. E-mail: naduvala@unlv.nevada.edu.

well-known “HO<sub>x</sub> dilemma”<sup>40</sup> which is one of the major issues surrounding hydroxyl chemistry in the middle atmosphere is linked to reactions (2)–(4). The “HO<sub>x</sub> dilemma” refers to the inability of photochemical models to accurately predict the abundance of OH and HO<sub>2</sub> above and below the stratopause (~45 km). This is, due in part, to the uncertainties in the rate coefficients of (2)–(4), believed to be as much as 50%. Though new sources of OH and HO<sub>2</sub> have been proposed based on nonequilibrium chemistry,<sup>37,38</sup> experimental data are lacking. As pointed out by Crutzen,<sup>41</sup> to resolve the “HO<sub>x</sub> dilemma” and the “ozone deficiency” (though controversial) major emphasis should be given to the reanalysis of the rate coefficients of (2)–(4). Since the rate coefficients of (1) and (2) are related through the equilibrium constant

$$K_{\text{eq}} = \frac{k_1}{k_2} \quad (6)$$

an accurate determination of the rate coefficient of (1) can provide accurate values of  $k_2$  or vice versa, provided the temperature dependence of the equilibrium constant is known precisely. Accurate determination of the equilibrium constant has been carried out recently. Troe and Ushakov<sup>14</sup> have suggested the following expression for  $K_{\text{eq}}$

$$K_{\text{eq}} = 17.0 \times (T/1000\text{K})^{-0.213} \exp(-8144\text{K}/T) \quad (7)$$

for temperatures in the range 1000–5000 K based on the most recent thermodynamical data.

Reaction (2) is also of considerable interest in astrochemistry in connection with interstellar oxygen chemistry.<sup>42</sup> The rate coefficients of (2) at temperatures as low as 100 K are required in modeling O<sub>2</sub> production by this process.

Most theoretical studies of the H + O<sub>2</sub> system have made use of the double many body expansion (DMBE IV) potential energy surface (PES) of Pastrana et al.<sup>8</sup> The accuracy of this potential has been questioned recently by Harding et al.<sup>13</sup> and Troe and Ushakov<sup>14</sup> who constructed a new ab initio PES for the H + O<sub>2</sub> system which is argued to be more accurate than the DMBE IV surface. Harding et al.<sup>13</sup> and Troe and Ushakov<sup>14</sup> reported rate coefficients for (2) using the new potential employing QCT calculations and statistical methods. Unfortunately, no quantum mechanical calculations are reported using this potential. In light of the HO<sub>x</sub> dilemma and the continuing interest in the H + O<sub>2</sub> reaction, we believe that it will be important to test the accuracy of the new PES for the HO<sub>2</sub> system using quantum mechanical calculations.

In this paper we report quantum mechanical calculations of the H + O<sub>2</sub> reaction on the DMBE IV and the Troe–Ushakov PESs. We focus on reaction 1 because benchmark quantum calculations on the DMBE IV PES (for  $J = 0$ )<sup>19</sup> are available. We limit our calculations to  $J = 0$  to reduce computational effort.

The paper is organized as follows. In section 2 we provide a brief description of the methodology. In section 3 we present results of our calculations on the two potential energy surfaces. Section 4 provides a summary and conclusions of our study.

## II. Method

We use the ABC reactive scattering program of Skouteris, Castillo, and Manolopoulos<sup>43</sup> to carry out the calculations. The program has been tested on a number of benchmark atom–diatom systems such as H + H<sub>2</sub>, Cl + H<sub>2</sub>, F + H<sub>2</sub>, and their isotopic counterparts. We have recently applied it to the study

of F + H<sub>2</sub><sup>44</sup> and F + HD<sup>45</sup> reactions at ultralow energies and the O + H<sub>2</sub> reaction at thermal energies.<sup>46</sup> All these reactions proceed via an abstraction mechanism. To the best of our knowledge, this is the first application of this program to a complex forming system such as the H + O<sub>2</sub> reaction. Details of the methodology are given elsewhere.<sup>43,47</sup>

Seideman and Miller<sup>48,49</sup> have shown that one can compute thermal rate coefficients directly from the cumulative reaction probabilities. This requires calculation of cumulative reaction probabilities  $N_J(E)$  for all contributing values of  $J$ . Unfortunately, there are only a handful of atom–diatom system for which this can be computed explicitly without requiring enormous computational capabilities. For the present system this is a very challenging task and would require massive computational effort. Since our aim is to compare the dynamics on the two PESs, we restrict our calculations to  $J = 0$ . One common approach to calculate  $N_J(E)$  from  $N_{J=0}(E)$  is to apply the  $J$ -shifting approach. The  $J$ -shifting approach is suitable for systems with a well-defined transition state. Since the H + O<sub>2</sub> reaction proceeds through HO<sub>2</sub> formation, it is not obvious what geometry should be used to apply the  $J$ -shifting method. However, based on calculations for nonzero  $J$  values using the coupled states method, Miller and co-workers<sup>27</sup> have found that the  $J$ -shifting method can be applied to the H + O<sub>2</sub> system if the transition-state geometry in the product valley is used instead of the H–O–O geometry corresponding to the HO<sub>2</sub> species. Here, we will adopt the  $J$ -shifting approximation with the [H–O···O]<sup>‡</sup> transition state located in the product valley in calculating thermal rate coefficients from  $N_{J=0}$ .

Thermal rate constants are computed from the cumulative reaction probability

$$N(E) = \sum_{J=0}^{\infty} (2J+1) N_J(E)$$

according to<sup>48,49</sup>

$$k(T) = \frac{1}{2\pi\hbar Q_{\text{mol}}(T)} \int_{-\infty}^{+\infty} dE e^{-E/k_B T} N(E) \quad (8)$$

where  $E$  is the total energy,  $k_B$  is the Boltzmann constant and,  $Q_{\text{mol}}$  is the molecular reactant partition function given by

$$Q_{\text{mol}}(T) = Q_{\text{el}}(T) Q_{\text{vib}}(T) Q_{\text{rot}}(T) Q_{\text{trans}}(T) \quad (9)$$

where  $Q_{\text{el}}(T)$ ,  $Q_{\text{vib}}(T)$ ,  $Q_{\text{rot}}(T)$ , and  $Q_{\text{trans}}(T)$  are, respectively, the electronic, vibrational, rotational, and translational partition functions.

Assuming that  $K$ , the projection of  $J$  on the body-fixed  $Z$  axis, is a good quantum number, and coriolis coupling is small, the  $J$ -shifting approximation for CRP becomes

$$N_J(E) \approx \sum_{K=-J}^J N_{JK}(E) \quad (10)$$

with

$$N_{JK}(E) \approx N_{J=0}(E - E_{JK}^{\ddagger}) \quad (11)$$

The last approximation implies that the reaction goes through a [H–O–O]<sup>‡</sup> transition-state geometry, and the rotational energy  $E_{JK}^{\ddagger}$  of the transition-state species is not sufficient to overcome the energy barrier for the reaction.<sup>48,49</sup> As mentioned above, this assumption is questionable for the present system because it assumes a well-defined transition state. For a symmetric top,

**TABLE 1: Convergence of Cumulative Reaction Probabilities with Respect to the Maximum Value of the Hyperradius at Which Boundary Conditions Are Applied<sup>a</sup>**

$E$ (eV)	$\rho_{\max}$	DMBE IV PES	Troe–Ushakov PES
		$N_{J=0}(E)$	$N_{J=0}(E)$
0.8170	25.05	1.26	
	30.05	1.29	
0.8440	25.05	1.24	1.72
	30.05	1.24	1.73
0.8755	25.05	2.38	3.17
	30.05	2.38	3.18
1.0200	25.05	3.60	5.08
	30.05	3.60	5.08
1.2200	25.05	5.53	7.10
	30.05	5.53	7.10
1.4200	25.05	9.47	12.25
	30.05	9.75	12.25

<sup>a</sup> For the DMBE IV potential,  $E_{\max} = 3.9$  eV,  $j_{\max} = 59$ , and  $N_{\max} = 933$ . For the Troe–Ushakov potential,  $E_{\max} = 4.2$  eV,  $j_{\max} = 59$ , and  $N_{\max} = 1151$ .

the rotational energy  $E_{JK}^{\ddagger}$  of the transition state is given by

$$E_{JK}^{\ddagger} = B^{\ddagger}J(J+1) + (A^{\ddagger} - B^{\ddagger})K^2 \quad (12)$$

where  $A^{\ddagger}$  and  $B^{\ddagger}$  are rotational constants.

With the  $J$ -shifting method the expression for the rate coefficient becomes

$$k(T) = \frac{Q_{\text{rot}}^{\ddagger}(T)}{2\pi\hbar Q_{\text{mol}}(T)} \int_{-\infty}^{+\infty} dE e^{-E/k_B T} N_{J=0}(E) \quad (13)$$

where  $Q_{\text{rot}}^{\ddagger}(T)$  is the rotational partition function of the transition-state complex:

$$Q_{\text{rot}}^{\ddagger}(T) = \sum_{J=0}^{\infty} (2J+1) \sum_{K=-J}^J e^{-E_{JK}^{\ddagger}/k_B T} \quad (14)$$

### III. Results

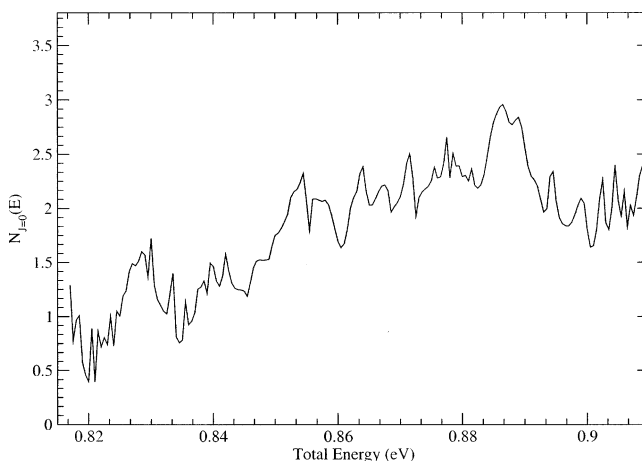
In this section we present reaction probabilities and rate coefficients for the H + O<sub>2</sub> reaction on the DMBE IV and Troe–Ushakov PESs to determine the sensitivity of the reaction dynamics to details of the potentials. First, we present convergence of the probabilities with respect to different parameters of the numerical solution of the Schrödinger equation for total energies ranging from the reaction threshold to 1.4 eV. The energy  $E$  is measured relative to the H + O<sub>2</sub> asymptote with  $E = 0$  taken to be the bottom of the H + O<sub>2</sub> well. Once the convergence is established we carry out calculations for over 200 energy values in the range of 0.82–1.4 eV to map out the resonance structures in the reaction probability. Finally, we provide a comparison between rate coefficients from the two potentials evaluated using the  $J$ -shifting approximation as well as results of previous experimental and theoretical works.

**A. Convergence Tests.** The details of the ABC program have been given elsewhere.<sup>43</sup> The Schrödinger equation is solved using the log-derivative method. Convergence of the cumulative reaction probabilities with respect to the hyperradius  $\rho$  is given in Table 1 for both the DMBE IV PES and the Troe–Ushakov PES for total energies ranging from the threshold value of 0.817 eV to 1.42 eV. It is seen that the value of  $\rho_{\max} = 30.05 a_0$  is adequate to secure convergence with respect to  $\rho_{\max}$  for both PESs in this energy range. Because of the slightly different energy spectrum for the diatomics in the Troe–Ushakov PES, the reaction channel is not open at the total energy value of 0.817 eV.

**TABLE 2: Convergence of the Cumulative Reaction Probabilities and Initial-State-Selected Reaction Probabilities with Respect to the Maximum Value of the Rotational Quantum Number  $j_{\max}$  for a Fixed Value of  $E_{\max} = 3.6$  eV on the DMBE PES<sup>a</sup>**

$E$	$j_{\max} = 49$ ( $N_{\max} = 729$ )		$j_{\max} = 59$ ( $N_{\max} = 823$ )		$j_{\max} = 69$ ( $N_{\max} = 910$ )	
	$N_{J=0}(E)$	$P_{0,1}(\text{tot})$	$N_{J=0}(E)$	$P_{0,1}(\text{tot})$	$N_{J=0}(E)$	$P_{0,1}(\text{tot})$
0.8170	1.28	2.8e-02	1.27	2.7e-02	1.27	2.7e-02
0.8440	1.26	1.6e-02	1.26	1.7e-02	1.26	1.7e-02
0.8755	2.29	6.2e-02	2.28	6.5e-02	2.28	6.5e-02
1.0200	3.57	9.8e-02	3.58	9.1e-02	3.58	9.1e-02
1.2200	5.54	1.1e-01	5.52	1.1e-01	5.52	1.1e-01
1.4200	9.83	3.2e-02	9.78	3.2e-02	9.78	3.2e-01

<sup>a</sup> The maximum number of channels  $N_{\max}$  is given in the brackets for each case.

**Figure 1.** Cumulative reaction probability as a function of the total energy for the H + O<sub>2</sub> reaction on the DMBE IV PES.

We have also checked the convergence of the results with respect to  $\rho_{\min}$  and  $\Delta\rho$ . Our test calculations show that values of  $\Delta\rho = 0.05 a_0$  and  $\rho_{\min} = 3.1 a_0$  are adequate to obtain converged results. Thus in our production calculations, we use  $\rho_{\min} = 3.1 a_0$ ,  $\rho_{\max} = 30.05 a_0$ , and  $\Delta\rho = 0.05 a_0$ . This requires a total of 539 steps in the log-derivative method.

Table 2 shows convergence tests with respect to the maximum number of rotational levels,  $j_{\max}$ , included in the calculations for the DMBE IV surface. The number of channels is determined by  $j_{\max}$  and  $E_{\max}$ , where  $E_{\max}$  is the cutoff energy for specifying the rovibrational basis set. Results are shown for  $j_{\max} = 49, 59$ , and 69 for a fixed value of  $E_{\max} = 3.6$  eV which led to maximum number of channels  $N_{\max} = 729, 823$ , and 910, respectively. We obtain converged values for both initial-state-selected reaction probabilities and cumulative reaction probabilities for  $j_{\max} = 59$  and 69 and we use  $j_{\max} = 59$  in our production calculations. Results in Table 2 also demonstrate that the cumulative reaction probabilities converge faster than the initial-state-selected reaction probabilities. Cumulative reaction probabilities in the energy range 0.817–0.9 eV are given in Figure 1 for the DMBE IV PES.

We carried out similar convergence studies on the Troe–Ushakov potential energy surface. It is interesting to point out that this PES has a different convergence property, and, in general, results converge less rapidly with the size of the basis set compared to the DMBE PES. Table 3 gives convergence of the CRP with respect to  $E_{\max}$  and  $j_{\max}$ . It is seen that results do not show a smooth convergence with respect to these parameters but oscillate around an average value with a deviation of around 10–12%. However, for the present purpose, we believe that

**TABLE 3: Convergence of the Cumulative Reaction Probabilities with Respect to  $j_{\max}$  and  $E_{\max}$  for the Troe–Ushakov PES<sup>a</sup>**

$E$	$j_{\max} = 49$ ( $N_{\max} = 115$ )	$j_{\max} = 59$ ( $N_{\max} = 1259$ )	$j_{\max} = 69$ ( $N_{\max} = 1397$ )	$E_{\max} = 4.2$ eV ( $N_{\max} = 1151$ )	$E_{\max} = 4.6$ eV ( $N_{\max} = 1385$ )
0.8270	0.87	0.90	0.92	0.96	0.98
0.8440	1.73	1.47	1.74	1.73	1.72
0.8755	3.23	3.07	2.86	3.19	3.00
1.0200	5.04	5.18	4.96	5.08	5.16
1.2200	7.48	7.17	7.07	7.10	7.33
1.4200	13.14	12.95	12.40	12.25	12.28

<sup>a</sup> The CRPs in the first three columns correspond to  $E_{\max} = 4.4$  eV. The last two columns show convergence with respect to  $E_{\max}$  for a fixed value of  $j_{\max} = 59$ .

**TABLE 4: Comparison of Cumulative Reaction Probabilities and Initial-State-Selected Reaction Probabilities for  $J = 0$  from the Present Study and Those of Pack et al.<sup>19</sup> Obtained Using the DMBE IV PES**

$E$ (eV)	present results		Pack et al. <sup>19</sup>	
	$N_{J=0}(E)$	$P_{0,1}(tot)$	$N_{J=0}(E)$	$P_{0,1}(tot)$
0.8170	1.29	2.54e-02	1.304	2.699e-02
0.8440	1.25	1.34e-02	1.262	2.169e-02
0.8755	2.38	6.24e-02	2.375	8.860e-02
1.0200	3.61	7.07e-02	3.592	7.779e-02
1.2200	5.63	1.59e-01	5.605	1.586e-01
1.4200	10.16	3.26e-01	10.012	3.348e-01

**TABLE 5: Transition-State Geometry and Corresponding Rotational Constants of the  $[\text{H}-\text{O}\cdots\text{O}]^\ddagger$  Species for the DMBE IV and the Troe–Ushakov PESs Used in the  $J$ -Shifting Approximation<sup>a</sup>**

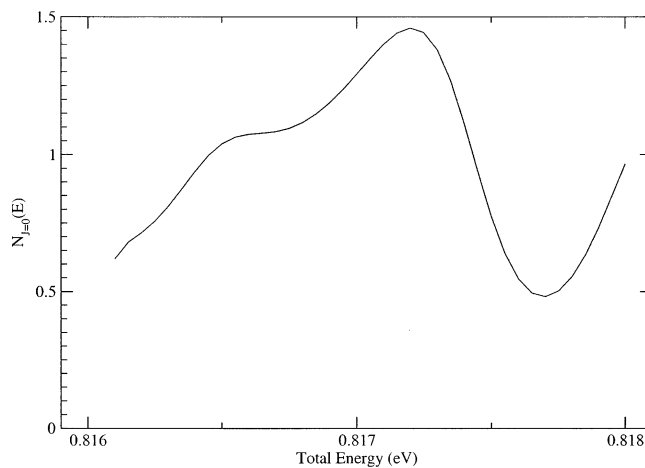
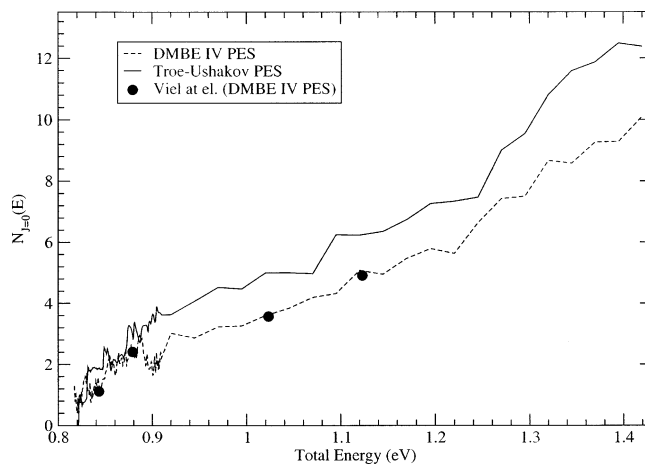
	$R_{\text{HO}}$	$R_{\text{OO}}$	$\widehat{\text{HOO}}$	$A^\ddagger$	$B^\ddagger$	$C^\ddagger$
Troe–Ushakov PES	1.85	5.47	45.26	35.98	0.249	0.248
DMBE IV PES <sup>22</sup>	1.82	5.08	40.00	44.92	0.289	0.288

<sup>a</sup> The DMBE results are taken from Viel et al.<sup>22</sup> Distances are in bohrs and rotational constants are in  $\text{cm}^{-1}$ .

the results are robust enough to make a meaningful comparison between the two PESs. It should also be mentioned that when calculating average quantities such as the thermal rate coefficient the resonances get washed out and small fluctuations in the CRP will not lead to significant errors in the rate coefficients.

As mentioned in section I, the  $\text{H} + \text{O}_2$  reaction has been the subject of a large number of theoretical calculations. Pack and co-workers<sup>19</sup> have carried out extensive convergence tests of the CRPs and initial-state-selected reaction probabilities on the DMBE IV PES using their version of hyperspherical coordinates. In Table 4 we provide an explicit comparison of our results with those of Pack et al.<sup>19</sup> for a number of energies ranging from the threshold value to 1.42 eV. Results of Pack et al.<sup>19</sup> are taken from Table 3 of their paper. It is seen that our calculations reproduce their converged results within 1% for the CRP. However, the agreement is less satisfactory for the initial-state-selected reaction probabilities, presumably due to the highly oscillating nature of the probabilities and their small magnitude.

Figure 2 shows the cumulative reaction probabilities computed on the DMBE PES in the narrow energy range of 0.816–0.818 eV to illustrate the smooth structure. This can be directly compared with Figure 4 of Pack et al.<sup>19</sup> In Figure 3 we compare the CRPs obtained with the DMBE IV and Troe–Ushakov PESs in the energy range of 0.81–1.42 eV. It is seen that both surfaces yield CRPs that are qualitatively similar, but the Troe–Ushakov potential leads to results that are 10–50% higher than that of the DMBE surface at energies above 0.9 eV. Viel et al.<sup>22</sup> reported CRP values on the DMBE surface using the flux correlation method of Miller and co-workers. Cumulative

**Figure 2.** Expanded view of the CRP  $N_{J=0}(E)$  showing its smooth behavior on a fine grid.**Figure 3.** Comparison of the cumulative reaction probabilities for the  $\text{H} + \text{O}_2$  reaction on the DMBE IV and the Troe–Ushakov PESs as functions of the total energy. The solid curve is the result on the Troe–Ushakov PES, and the broken curve is the result obtained using the DMBE IV PES. The results of Viel et al.<sup>22</sup> are shown by the filled circles.

reaction probabilities taken from Table 4 of Viel et al.<sup>22</sup> are also included in Figure 3, and they are in good agreement with our results.

**B. Rate Coefficients.** Although one can compute the  $J = 0$  contribution to the thermal rate coefficient exactly from  $N_{J=0}(E)$  this contribution to the rate coefficient is very small. For the  $\text{H} + \text{O}_2$  reaction contributions from  $J = 0-100$  are required in accurately evaluating the rate coefficients for temperatures lower than 2000 K. Such calculations require massive computational effort and are beyond the scope of this paper. Our comparison of CRPs on the widely used DMBE IV PES and the newer Troe–Ushakov PES shows that further refinement of the PES is required for the present system. Though

**TABLE 6: Thermal Rate Coefficients in  $\text{cm}^3 \text{Molecule}^{-1} \text{s}^{-1}$  for the  $\text{H} + \text{O}_2 \rightarrow \text{OH} + \text{O}$  Reaction**

$T$ (K)	present results		Skinner et al. <sup>27</sup>		experiment <sup>5</sup>
	DMBE IV PES	Troe–Ushakov PES	$J$ -shifting	HCA	
600	$1.43 \times 10^{-16}$	$2.21 \times 10^{-16}$	$3.39 \times 10^{-16}$	$4.12 \times 10^{-16}$	$6.34 \times 10^{-16}$
700	$1.09 \times 10^{-15}$	$1.71 \times 10^{-15}$			$3.76 \times 10^{-15}$
1000	$4.22 \times 10^{-14}$	$6.87 \times 10^{-14}$	$9.03 \times 10^{-14}$	$10.3 \times 10^{-14}$	$9.23 \times 10^{-14}$
1200	$1.76 \times 10^{-13}$	$2.88 \times 10^{-13}$			$3.2 \times 10^{-13}$
1500	$7.32 \times 10^{-13}$	$1.21 \times 10^{-12}$			$1.11 \times 10^{-12}$
2000	$3.07 \times 10^{-12}$	$5.06 \times 10^{-12}$			$3.87 \times 10^{-12}$
2500	$7.21 \times 10^{-12}$	$11.80 \times 10^{-12}$			$8.16 \times 10^{-12}$

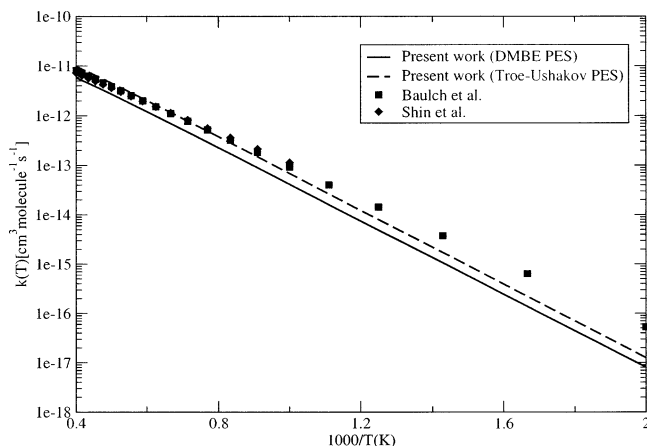


**Figure 4.** Comparisons of rate coefficients of the  $\text{H} + \text{O}_2 \rightarrow \text{OH} + \text{O}$  reaction from the present study with experimental data. Solid line: results of present calculations on the DMBE IV PES; broken line: results of present calculations on the Troe–Ushakov PES; filled squares: experimental data from Baulch et al.;<sup>5</sup> filled diamonds: experimental data of Shin and Michael.<sup>50</sup>

the  $J$ -shifting approximation is not expected to be very accurate for this system, it will be interesting to compare the rate coefficients from the two potential surfaces using this approach. Miller and co-workers<sup>22,26,27</sup> have also used the  $J$ -shifting approach in calculating the rate coefficient but with a completely different numerical method for solving the Schrödinger equation.

The validity of the  $J$ -shifting approach depends on the choice of the transition-state geometry used in the  $J$ -shifting approximation. Based on comparisons with more accurate quantum calculations, Viel et al.<sup>22</sup> and Skinner et al.<sup>27</sup> showed that the transition-state  $[\text{H}-\text{O}\cdots\text{O}]^\ddagger$  located in the product channel yields results that are in better agreement with experiments. This appears to be justified in this case because the reaction can be viewed as the motion of a light atom around a heavy diatomic molecule that is dissociating. The geometries of various  $\text{HO}_2$  complexes and corresponding rotational constants are given in Table 5 of Viel et al.<sup>22</sup> for the DMBE PES. We have computed the geometry and rotational constants of the  $[\text{H}-\text{O}\cdots\text{O}]^\ddagger$  transition state for the Troe–Ushakov PES required for the  $J$ -shifting approximation. These values along with the corresponding values for the DMBE PES given by Viel et al.<sup>22</sup> are listed in Table 5. It is seen that the rotational constants are about 15–20% lower for the Troe–Ushakov PES implying that the transition state lies further out in the product valley for the Troe–Ushakov PES. The  $\text{O}\cdots\text{O}$  bond distance at the transition state for the DMBE PES is 2.69 Å compared to 2.90 Å for the Troe–Ushakov PES.

In Figure 4 we compare rate coefficients for the  $\text{H} + \text{O}_2$  reaction from our calculations using the two PESs with experimental data from Baulch et al.<sup>5</sup> and Shin and Michael.<sup>50</sup> The rotational constants listed in Table 5 are used in applying the  $J$ -shifting approximation for computing the rate coefficients. For the evaluation of the rotational partition function  $Q_{\text{rot}}^\ddagger$  we

have included  $J = 0-200$  in eq 14. The electronic partition function  $Q_{\text{el}}$  for  $\text{H} + \text{O}_2$ <sup>22</sup> was taken to be 3. The data from Baulch et al.<sup>5</sup> correspond to the best fit to a collection of experimental data. It is seen that at temperatures below 1000 K the  $J$ -shifting calculations on the DMBE PES yield rate coefficients that are significantly lower than the experimental results. Between 1000 and 2500 K, the DMBE results are within a factor of 2 of the experimental results with close agreement with experiment at the high temperature end. The agreement with experiment is much better for the Troe–Ushakov PES. In particular, results on the Troe–Ushakov PES differ only by 10–40% of the experimental values in the temperature range of 1000–2500 K.

In Table 6 we list rate coefficients from our calculations on the two PESs and experimental data from Baulch et al.<sup>5</sup> in the temperature range of 600–2500 K. We also include rate coefficients at 600 and 1000 K obtained by Skinner et al.<sup>27</sup> on the DMBE surface using the  $J$ -shifting approximation and the helicity conserving approximation (HCA). The  $J$ -shifted results of Skinner et al.<sup>27</sup> are in close agreement with the presumably more accurate helicity conserving approximation. Our results on the DMBE PES are about a factor of 2 smaller than those of Skinner et al.<sup>27</sup> We do not know the source of this discrepancy.

#### IV. Summary and Conclusions

In this paper, we provide the first detailed comparison between the DMBE IV PES and the Troe–Ushakov PES for the  $\text{H} + \text{O}_2$  reaction using quantum dynamics calculations. Our calculations show that results are sensitive to details of the PES. Rate coefficients are evaluated using a  $J$ -shifting approximation. The Troe–Ushakov PES gives rate coefficients that are about 50% larger than those of the DMBE surface. Comparison with experimental data shows that the  $J$ -shifting approximation works reasonably well for the  $\text{H} + \text{O}_2$  reaction at temperatures above 1000 K and that the Troe–Ushakov potential surface provides improved agreement with experiment than the DMBE surface. Our results are consistent with the findings of Goldfield and Meijer<sup>30</sup> that the DMBE PES significantly underestimates the absolute value of the cross sections compared to experimental results.<sup>6</sup> Clearly, more accurate calculations that do not use the  $J$ -shifting approximation and that include the effect of recombination and nonadiabatic effects are required for a quantitative comparison with experimental data. The effect of recombination is especially important at lower temperatures. The open shell character of the OH molecule and geometric phase effect<sup>20</sup> should also be considered in a full description of the dynamics. We expect that calculations that include all these effects will become feasible soon and that the present study will stimulate calculations of more accurate potential energy surfaces for the  $\text{HO}_2$  system.

**Acknowledgment.** We dedicate this paper to Gert Due Billing, whose work continues to inspire us all. This work was supported by the National Science Foundation through Grant #

ATM-0205199. We thank Antonio Varandas for useful discussions and Jurgen Troe for providing us the program to compute the H + O<sub>2</sub> potential energy surface. We also thank Claude Leforestier and Bill Miller for useful discussions.

### References and Notes

- (1) Klienermanns, K.; Wolfrum J. *J. Chem. Phys.* **1984**, *80*, 1446.
- (2) Miller, J. A.; Kee R. J.; Westbrook C. K. *Annu. Rev. Phys. Chem.* **1990**, *41*, 345.
- (3) Kessler K.; Klienermanns, K. *J. Chem. Phys.* **1992**, *97*, 374.
- (4) Seeger, S.; Sick, V.; Volpp, H.-R.; Wolfrum, J. *Isr. J. Chem.* **1994**, *34*, 5.
- (5) Baulch, D. L. et al. *J. Phys. Chem. Ref. Data* **1994**, *23*, 847.
- (6) Bajeh M. A. et al. *J. Phys. Chem. A* **2001**, *105*, 3359.
- (7) Miller, J. A. *J. Chem. Phys.* **1986**, *84*, 6170.
- (8) Pastrana, M. R.; Quintales, L. A. M.; Brandão, J.; Varandas, A. J. *C. J. Phys. Chem.* **1990**, *94*, 8073.
- (9) Nyman, G.; Davidsson, J. *J. Chem. Phys.* **1990**, *92*, 2415.
- (10) Varandas, A. J. C.; Brandão, J.; Pastrana, M. R. *J. Chem. Phys.* **1990**, *96*, 5137.
- (11) Varandas, A. J. C. *Mol. Phys.* **1995**, *85*, 1159.
- (12) Varandas, A. J. C. *Chem. Phys. Lett.* **1995**, *235*, 111.
- (13) Harding, L. B.; Maergoiz, A. I.; Troe, J.; Ushakov, V. G. *J. Chem. Phys.* **2000**, *113*, 11019.
- (14) Troe, J.; Ushakov, V. G. *J. Chem. Phys.* **2001**, *115*, 3621.
- (15) Marques, J. M. C.; Varandas, A. J. C. *Phys. Chem. Chem Phys.* **2001**, *3*, 505.
- (16) Harding, L. B.; Troe, J.; Ushakov, V. G. *Phys. Chem. Chem Phys.* **2001**, *3*, 2630.
- (17) Marques, J. M. C.; Varandas, A. J. C. *Phys. Chem. Chem Phys.* **2001**, *3*, 2632.
- (18) Pack, R. T.; Butcher, E. A.; Parker, G. A. *J. Chem. Phys.* **1993**, *99*, 9310.
- (19) Pack, R. T.; Butcher, E. A.; Parker, G. A. *J. Chem. Phys.* **1995**, *102*, 5998.
- (20) Kendrick, B.; Pack, R. T. *J. Chem. Phys.* **1996**, *104*, 7475.
- (21) Leforestier, C.; Miller, W. H. *J. Chem. Phys.* **1994**, *100*, 733.
- (22) Viel, A.; Leforestier, C.; Miller, W. H. *J. Chem. Phys.* **1998**, *108*, 3489.
- (23) Groenenboom, G. C. *J. Chem. Phys.* **1998**, *108*, 5677.
- (24) Zhang, D. H.; Zhang, J. Z. *J. Chem. Phys.* **1994**, *101*, 3671.
- (25) Yang, C.-Y.; Klippenstein, S. J. *J. Chem. Phys.* **1995**, *103*, 7287.
- (26) Germann, T. C.; Miller, W. H. *J. Phys. Chem. A* **1997**, *101*, 6358.
- (27) Skinner, D. E.; Germann, T. C.; Miller, W. H. *J. Phys. Chem. A* **1998**, *102*, 3828.
- (28) Meijer, A. J. H. M.; Goldfield, E. M. *J. Chem. Phys.* **1998**, *108*, 5404.
- (29) Meijer, A. J. H. M.; Goldfield, E. M. *J. Chem. Phys.* **1999**, *110*, 870.
- (30) Goldfield, E. M.; Meijer, A. J. H. M. *J. Chem. Phys.* **2000**, *113*, 11055.
- (31) Meijer, A. J. H. M.; Goldfield, E. M. *Phys. Chem. Chem. Phys.* **2001**, *3*, 2811.
- (32) Zhang, H.; Smith, S. C. *J. Chem. Phys.* **2002**, *116*, 2354.
- (33) Zhang, H.; Smith, S. C. *J. Chem. Phys.* **2002**, *117*, 5174.
- (34) Gonzalez-Lezema, T.; Rackham, E. J.; Manolopoulos, D. E. *J. Chem. Phys.* **2004**, *120*, 2247.
- (35) Jucks, K. W. et al. *Geophys. Res. Lett.* **1998**, *25*, 3935.
- (36) Conway, R. R. et al. *Geophys. Res. Lett.* **2000**, *27*, 2613.
- (37) Varandas, A. J. C. *Eur. J. Chem. Phys. Phys. Chem.* **2002**, *3*, 433.
- (38) Varandas, A. J. C. *J. Phys. Chem. A* **2004**, *108*, 758.
- (39) Robertson, R.; Smith, G. P. *Chem. Phys. Lett.* **2002**, *358*, 157.
- (40) Summers, M. E. et al. *Science* **1997**, *277*, 1967.
- (41) Crutzen, P. J. *Science* **1997**, *277*, 1951.
- (42) Viti, S.; Roueff, E.; Hartquist, T. W.; Pineau des Forêts, G.; Williams, D. A. *Astron. Astrophys.* **2001**, *370*, 557.
- (43) Scouteris, D.; Castillo, J. F.; Manolopoulos, D. E. *Comput. Phys. Commun.* **2000**, *133*, 128.
- (44) Balakrishnan, N.; Dalgarno, A. *Chem. Phys. Lett.* **2001**, *341*, 652; **2002**, *351*, 159.
- (45) Balakrishnan, N.; Dalgarno, A. *J. Phys. Chem. A* **2003**, *107*, 7101.
- (46) Balakrishnan, N. *J. Chem. Phys.* **2003**, *119*, 195.
- (47) Schatz, G. C. *Chem. Phys. Lett.* **1988**, *150*, 92.
- (48) Seideman, T.; Miller, W. H. *J. Chem. Phys.* **1992**, *96*, 4412.
- (49) Seideman, T.; Miller, W. H. *J. Chem. Phys.* **1992**, *97*, 2499.
- (50) Shin, K. S.; Michael, J. V. *J. Chem. Phys.* **1991**, *95*, 262.